# Finite-volume matrix Hamiltonian model for a $\Delta \to N\pi$ system

J. M. M. Hall,[1] A. C.-P. Hsu,[1] D. B. Leinweber,[1] A. W. Thomas,[1,2] and R. D. Young[1,2]

[1]*Special Research Centre for the Subatomic Structure of Matter (CSSM), School of Chemistry and Physics,*
*University of Adelaide, Adelaide, South Australia 5005, Australia*
[2]*ARC Centre of Excellence for Particle Physics at the Terascale, School of Chemistry and Physics,*
*University of Adelaide, Adelaide, South Australia 5005, Australia*

A matrix Hamiltonian model is developed to address the finite-volume effects appearing in studies of baryon resonances in lattice QCD. The Hamiltonian model includes interaction terms in a transparent way and can be readily generalized to address multichannel problems. The eigenvalue equation of the model is exactly solvable and can be matched onto chiral effective field theory. The model is investigated in the case of $\Delta \to N\pi$ scattering. A robust method for determining the resonance parameters from lattice QCD is developed. It involves constraining the free parameters of the model based on the lattice spectrum in question. The method is tested in the context of a set of pseudodata, and a picture of the model dependence is obtained by examining a variety of regularization schemes in the model. A comparison is made with the Lüscher method, and it is found that the matrix Hamiltonian method is equally robust. Both methods are tested in a more realistic scenario, where a background interaction corresponding to direct $N\pi \leftrightarrow N\pi$ scattering is incorporated into the pseudodata. The resulting extraction of the resonance parameters associated with the $\Delta$ baryon resonance provides evidence that an effective field theory style of approach yields a successful realization of finite-volume effects in the context of baryon resonances.

## I. INTRODUCTION

The behavior of the excited states of baryons represents an important research topic in nuclear and particle physics. The extraction of resonance parameters (e.g., masses and widths) provides insight into the scattering behavior of hadronic interactions. Lattice QCD constitutes a principal tool for the analysis of nonperturbative physics; however, observables must be computed in a finite volume. Finite-volume models of hadronic interactions represent a valuable avenue for investigating the intrinsic features of lattice QCD. They assist in the interpretation of discrete eigenstates in relation to the asymptotic behavior of the $S$ matrix measured in experiments. Recent advances in lattice QCD have enabled the extraction of the lowest-lying excitation energies [1–5]. However, the extraction of resonance parameters from multihadron interactions presents an ongoing challenge for current research [6–16].

In this article, a finite-volume matrix Hamiltonian model is introduced, which is exactly solvable. A matrix is constructed, and its entries are populated with energies corresponding to different momentum states of the interaction channel(s). The solution of the eigenvalue equation takes the form of a one-loop renormalization formula for a bare resonance energy, reminiscent of finite-volume chiral effective field theory ($\chi$EFT). The Hamiltonian can then be matched onto the corresponding $\chi$EFT formula by choosing the form of the interaction in the model. A property of the formalism is the ability to reproduce the "avoided level crossing" observed in lattice QCD calculations, while also being able to reproduce the appropriate continuum limit of $\chi$EFT. Thus the physical behavior of the energy eigenvalues

near a resonance due to the mixing of the particle states can be estimated. Furthermore, the Hamiltonian method lends itself to an intuitive generalization in addressing multichannel problems, with the inclusion of additional degrees of freedom, corresponding to the new interactions.

The matrix Hamiltonian formalism is applied to $\Delta \to N\pi$ decay, and its energy spectrum is generated for a range of finite box sizes, $L$. A method for extracting the resonance parameters from a lattice QCD spectrum is then postulated, which involves fitting the free parameters of the model. The method is tested by generating a set of pseudodata from the model itself. The pseudodata are analyzed with an alternative version of the model and a selection of different regularization parameters. This provides an indication of the model dependence in correctly obtaining the resonance position. The success of the identification of the phase shift is compared to that of the Lüscher method [17]. This serves to establish a benchmark for the Hamiltonian model in obtaining the resonance position. It is found that the matrix Hamiltonian model, as applied to $\Delta \to N\pi$ decay, is of comparable accuracy to the Lüscher method.

## II. SCATTERING THEORY FROM EFFECTIVE FIELD THEORY

In continuum scattering theory, below inelastic thresholds, amplitudes of the partial-wave decomposition of the wave function, which are complex valued, may be converted into a real-valued number called the phase shift, $\delta_l(k)$, by exploiting the conservation of angular momentum. The phase shift, which depends on the orbital angular

momentum $l$ and external momentum $k$, is related to the total cross section of a scattering process, via

$$\sigma(k) = \int d\Omega |f(k, \theta)|^2, \tag{1}$$

where

$$f(k, \theta) = \sum_l (2l + 1) P_l(\cos \theta) \frac{e^{i\delta_l(k)} \sin \delta_l(k)}{k}, \tag{2}$$

where $P_l$ is the $l$th Legendre polynomial. The external momentum of a particle with mass $m$ is related to the external energy by $k = \sqrt{E^2 - m^2}$. In the case of $P$-wave scattering ($l = 1$), the total cross section simplifies to the form

$$\sigma(k) = 4\pi \frac{3\sin^2 \delta(k)}{k^2}, \tag{3}$$

where $\delta(k) \equiv \delta_1(k)$. The energy at which the phase shift passes through 90° is the resonance energy, $E_{res}$.

The investigation of $\Delta \to N\pi$ decay is of particular interest. It provides insight into the $\Delta$ resonance of $N\pi$ scattering: an archetypal example of a baryon resonance. The on-shell $t$ matrix associated with $N\pi$ scattering from a $\Delta$ baryon, $T \equiv t(k, k; E^+)$, can be obtained by solving the Lippmann-Schwinger equation, and the phase shift is directly related to the $t$ matrix, via

$$T = \frac{g_{\Delta N}^2(k)}{E - \Delta_0 - \Sigma_{\Delta N}(k)} \tag{4}$$

$$= -\frac{1}{\pi k E} e^{i\delta(k)} \sin \delta(k). \tag{5}$$

The quantity $\Delta_0$ represents the bare value of the resonance energy, which becomes renormalized by the one-pion loop integral, $\Sigma_{\Delta N}(k)$ (shown in Fig. 1), and may be chosen such that $E_{res}$ matches the phenomenological value, $E_{res}^{phys} = 292$ MeV. By working in the heavy-baryon approximation, the kinetic energy of the nucleon is neglected in this simple model, and calculations may be performed relative to the nucleon mass. Thus, the external energy may be expressed in terms of the pion energy, $E = \omega_\pi(k)$.

The coupling $g_{\Delta N}(k)$ takes the following form, as obtained from $\chi$EFT,
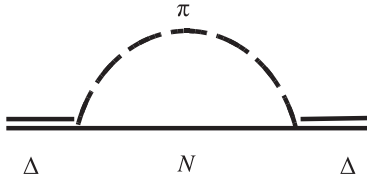


FIG. 1. The leading-order one-pion loop contribution to the resonance energy $E$ associated with $\Delta \to N\pi$ decay. All charge conserving transitions are implicit.

$$g_{\Delta N}^2(k) = \chi_\Delta \frac{2}{\pi} \frac{k^2 u^2(k)}{\omega_\pi(k)}, \tag{6}$$

where the coefficient $\chi_\Delta$ is defined in terms of known phenomenological parameters: $f_\pi = 92.4$ MeV and $\mathcal{C} = -1.52$, as derived from the SU(6) flavor-symmetry relation

$$\chi_\Delta = \frac{3}{32\pi f_\pi^2} \frac{2}{9} \mathcal{C}^2. \tag{7}$$

The parameters $f_\pi$ and $\mathcal{C}$ occur in the first-order interaction Lagrangian of chiral perturbation theory ($\chi$PT) describing the $\Delta \to N\pi$ interaction [18–23]

$$\mathcal{L}_{\chi PT} = -\frac{\mathcal{C}}{2f_\pi} \bar{N} T^a \gamma^{\mu\nu} \Delta_\nu \partial_\mu \pi^a + \text{H.c.}, \tag{8}$$

where $T^a$ are the relevant $2 \times 4$ isospin transition matrices [24].

Note that a finite-range regulator $u(k)$ has been introduced into the coupling term of Eq. (6). This serves to control the otherwise ultraviolet divergent loop integral and, in addition, will be used in Sec. III to establish a finite interaction range in the Hamiltonian model. For more detailed discussions of finite-range regularization, see Refs. [25–29].

The leading-order pion loop integral shown in Fig. 1 takes the form

$$\Sigma_{\Delta N}(k) = \int_0^\infty dk' \frac{k'^2 g_{\Delta N}^2(k')}{\omega_\pi(k) - \omega_\pi(k') - i\epsilon} \tag{9}$$

$$= \chi_\Delta \frac{2}{\pi} \mathcal{P} \int_0^\infty dk' \frac{k'^4 u^2(k')}{\omega_\pi(k')[\omega_\pi(k) - \omega_\pi(k') - i\epsilon]}, \tag{10}$$

where $\mathcal{P}$ indicates that a principal value integral must be performed. By using Eq. (5), it is straightforward to solve for $\delta(k)$. A plot of the phase shift against external energy, $E = \omega_\pi(k)$, is shown in Fig. 2, which takes the form of a Breit-Wigner-like curve.

## III. FINITE-VOLUME HAMILTONIAN MODEL

In the following finite-volume heavy-baryon model, a matrix Hamiltonian is defined to include the interaction between the $\Delta$ baryon and the pion-nucleon system. The rows and columns of $H$ represent the total three-momentum values available to the pion ($k_1 = 2\pi/L, k_2 = 4\pi/L \ldots$). In the simplest version of the model, the $N\pi$ states only couple to the $\Delta$ baryon.

The Hamiltonian may be written as the sum of free and interaction Hamiltonians, $H = H_0 + H_I$. The free Hamiltonian $H_0$ takes the form
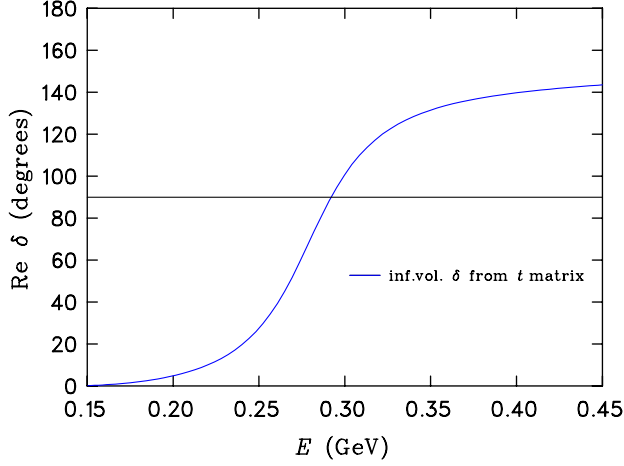
FIG. 2 (color online).   The infinite-volume phase shift $\delta$ associated with elastic $N\pi$ scattering via a $\Delta$ baryon intermediate state, plotted against the external pion energy $E$ (where $E_{\text{tot}} = M_N + E$), as calculated from the on-shell $t$ matrix of Eq. (5).

$$H_0 = \begin{pmatrix} \Delta_0 & 0 & 0 & \cdots \\ 0 & \omega_\pi(k_1) & 0 & \cdots \\ 0 & 0 & \omega_\pi(k_2) & \\ \vdots & \vdots & & \ddots \end{pmatrix}, \quad (11)$$

where $\omega_\pi(k_n) \equiv \sqrt{k_n^2 + m_\pi^2}$ is the pion energy, and the pion momenta at finite volume take only the discrete values available in a box of length $L$, obeying the condition $k_n^2 = (\frac{2\pi}{L})^2 n$ for a squared integer $n \equiv n_x^2 + n_y^2 + n_z^2$. $H_0$ has nonzero diagonal entries representing the noninteracting energy of a pion at certain values of momentum. The nucleon recoil energy vanishes in the heavy-baryon limit. The first element of $H_0$ represents the bare resonance mass relative to the nucleon mass, $\Delta_0$. The value of $\Delta_0$ is chosen so that the resonance position takes the phenomenological value 292 MeV, in the infinite-volume case in Eq. (4).

The interacting Hamiltonian $H_I$ contains couplings $g_{\Delta N}$ in the top row and left-most column,

$$H_I = \begin{pmatrix} 0 & g_{\Delta N}^{\text{fin}}(k_1) & g_{\Delta N}^{\text{fin}}(k_2) & \cdots \\ g_{\Delta N}^{\text{fin}}(k_1) & 0 & 0 & \cdots \\ g_{\Delta N}^{\text{fin}}(k_2) & 0 & 0 & \cdots \\ \vdots & \vdots & \vdots & \ddots \end{pmatrix}. \quad (12)$$

This represents the interaction between the bare $\Delta$ baryon and the $N\pi$ system over a range of momentum values. The couplings are chosen to take a similar form to that of Eq. (6) but contain additional factors relevant to the normalization of the discrete momenta in a finite-volume box,

$$g_{\Delta N}^{\text{fin}}(k_n) = \sqrt{\frac{C_3(n)}{4\pi}} \left(\frac{2\pi}{L}\right)^{3/2} g_{\Delta N}(k_n). \quad (13)$$

Note that the cubic symmetry of the system means that each nonzero $n$ need occur only once in the rows and

columns of $H$, so long as the finite-volume couplings $g_{\Delta N}^{\text{fin}}(k_n)$ contain the appropriate normalization factor $\sqrt{C_3(n)}$, where $C_3(n)$ represents the number of ways of summing the squares of three integers to equal $n$.

For the purposes of this model, $u(k_n)$ is chosen to take the form of a dipole regulator, with a regularization scale of $\Lambda = 0.8$ GeV,

$$u(k_n) = \left(1 + \frac{k_n^2}{\Lambda^2}\right)^{-2}. \quad (14)$$

However, in Sec. V, the associated model dependence of the choice of regulator on the extraction of the resonance parameters from the model is investigated and a variety of regularization schemes are examined.

The eigenvalues of the Hamiltonian matrix correspond to the different energy levels in a finite volume and may be calculated for a range of $L$ values. The ten lowest energy levels as a function of $L$ are shown in Fig. 3, with the noninteracting energies shown as dotted lines.

The Hamiltonian model, by construction, matches onto the $\chi$EFT formula for the renormalization of the resonance mass in a finite volume. The eigenvalue equation of the Hamiltonian, $\det(H - \lambda\mathbb{1}) = 0$, can be solved exactly and takes the form

$$\lambda = \Delta_0 - \sum_{n=1}^{\infty} \frac{(g_{\Delta N}^{\text{fin}}(k_n))^2}{\omega_\pi(k_n) - \lambda} \quad (15)$$

$$= \Delta_0 - \frac{\chi_\Delta}{2\pi^2} \left(\frac{2\pi}{L}\right)^3 \sum_{n=1}^{\infty} C_3(n) \frac{k_n^2 u^2(k_n)}{\omega_\pi(k_n)[\omega_\pi(k_n) - \lambda]}. \quad (16)$$

A comparison with Eq. (10) shows that the sum term takes the same form as the loop integral, upon the restoration of the continuum integral
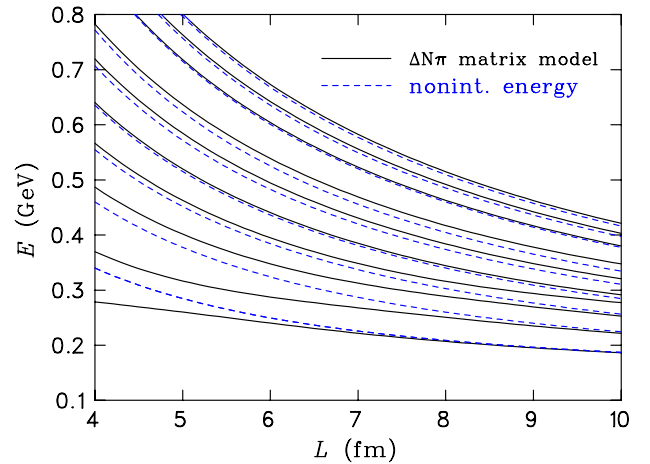


FIG. 3 (color online).   The lowest-lying energy levels from the $\Delta N\pi$ model, described in Eqs. (11)–(14) (solid lines), and the corresponding noninteracting energies (dotted lines).

$$\left(\frac{2\pi}{L}\right)^3 \sum_{n=1}^{\infty} C_3(n) \rightarrow \int \mathrm{d}^3 k. \qquad (17)$$

This correspondence is a consequence of the judicious choice of the form of the coupling in the finite-volume Hamiltonian $g_{\Delta N}^{\mathrm{fin}}$.

The subtle, yet important difference between Eqs. (10) and (16) is that the energy eigenvalue $\lambda$ appears on both sides of the equation derived from the Hamiltonian. The presence of $\lambda$ in the denominator, whose solution must be finite, results in the avoided level crossing observed in lattice QCD, where the resonance energy corresponds to maximal mixing of the single-particle and multiparticle states. That is, the correct quantum mechanical behavior of the multiparticle system is directly built into the Hamiltonian model. This is the finite-volume analogue of the principal value integral in the continuum theory.

The Hamiltonian model may be extended to include a direct $N\pi \leftrightarrow N\pi$ interaction, which could be viewed as an approximation to the Chew-Low interaction. For example, one can add additional terms in the interaction matrix, $H_I$:

$$g_{\mathrm{CL}}(k_i, k_j) = -g_{N\pi}(k_i) g_{N\pi}(k_j) \frac{1}{\sqrt{\omega_\pi(k_i) \omega_\pi(k_j)}}. \qquad (18)$$

In the cloudy bag model [30,31], the couplings $g_{N\pi}$ and $g_{\Delta N}^{\mathrm{fin}}$ are related by the equation $g_{N\pi}(k_i) = \kappa g_{\Delta N}^{\mathrm{fin}}(k_i)$ with a ratio $\kappa = \sqrt{25/18}$ estimated from SU(6) symmetry. In the case of the $t$ matrix, the Lippmann-Schwinger equation with a rank-2 separable potential can be solved as per Mongan [32].

This additional interaction will be used to test the model independence in the procedure of extracting the phase shift in Sec. V. The comparison of two models, one with extra background interactions of the form of Eq. (18) and one without the extra interactions, will provide insight into the robustness of the identification of resonance parameters from an effective model.

## IV. PHASE SHIFT EXTRACTION FROM THE LATTICE

The identification of resonance parameters in a finite volume is important for interpreting lattice QCD results in the light of experiment. The connection between the energy spectra of lattice QCD simulations and the asymptotic states of the $S$ matrix represents a current challenge for research in finite-volume hadron spectroscopy [6,33–36].

The features of the Hamiltonian model are ideally suited to the extraction of resonance parameters from lattice QCD energy spectra. Not only is the construction of the Hamiltonian transparent and intuitive in terms of the potentials one chooses to include, but the formalism may be easily generalized to include multiple channels. By generating energy eigenvalues from a Hamiltonian model, such as those shown in Fig. 3 for the $\Delta \rightarrow N\pi$ interaction,

the free parameters of the model may be tuned to fit the energy spectrum of a lattice QCD calculation. In the case of the $\Delta \rightarrow N\pi$ model, this entails minimizing the chi-square for the parameters $\chi_\Delta$ and $\Delta_0$. The resonance energy and phase shift may then be extracted by using the fitted values of the parameters, input into Eq. (5). An infinite-volume phase shift, much like that of Fig. 2, is thus obtained, except that the underlying parameters have been extracted directly from lattice QCD results.

## V. COMPARISON WITH THE LÜSCHER METHOD

In order to demonstrate the success of the Hamiltonian method in reproducing accurate phase shifts from the finite-volume energy spectrum of the model, a comparison is made with the well-known Lüscher method [17]. Lüscher's formula describes a fixed relationship between the scattering phase shift $\delta$ and the momentum corresponding to the $j$th energy level in a finite volume

$$\delta(k_j; L) = j\pi - \phi\left(\frac{k_j L}{2\pi}\right). \qquad (19)$$

The kinematic function $\phi(q)$ takes the form of a three-dimensional Zeta-like function (which must be regularized in an appropriate fashion), defined in terms of dimensionless lattice momenta, $q \equiv kL/(2\pi)$,

$$\phi(q) = -\arctan\left(\frac{\pi^{3/2} q}{Z_{00}(1, q^2)}\right), \qquad (20)$$

$$Z_{00}(1, q^2) = \frac{1}{\sqrt{4\pi}} \sum_{\vec{n} \in \mathbb{Z}^3} \frac{1}{\vec{n}^2 - q^2}. \qquad (21)$$

The momenta corresponding to a lattice energy spectrum may be input into Lüscher's formula to obtain volume-dependent "phase shifts" $\delta(k_j; L)$.

As an example, consider the application of the Lüscher method to the energy spectrum of the $\Delta \rightarrow N\pi$ model, treating the spectrum as pseudodata. By taking the momenta associated with the energy eigenvalues, shown in Fig. 3, as inputs, and choosing a particular box size $L$, the finite-volume estimates of the phase shifts may be compared with the known infinite-volume phase shifts, as shown in Fig. 2. The result is plotted on the same axes, in Fig. 4, for a range of box sizes. Both the infinite-volume phase shift and the Hamiltonian energy spectrum are generated using a dipole regulator with $\Lambda = 0.8$ GeV. Figure 4 shows that the finite-volume corrections associated with applying the Lüscher method to a finite-volume effective Hamiltonian model are insignificant for $L \geq$ 3 fm at the physical pion mass. It will be demonstrated that the matrix Hamiltonian method of obtaining a phase shift from finite-volume energy levels is comparable with the Lüscher method.

Note that, in using Lüscher's method, an interpolation function must be chosen in order to obtain the pole position
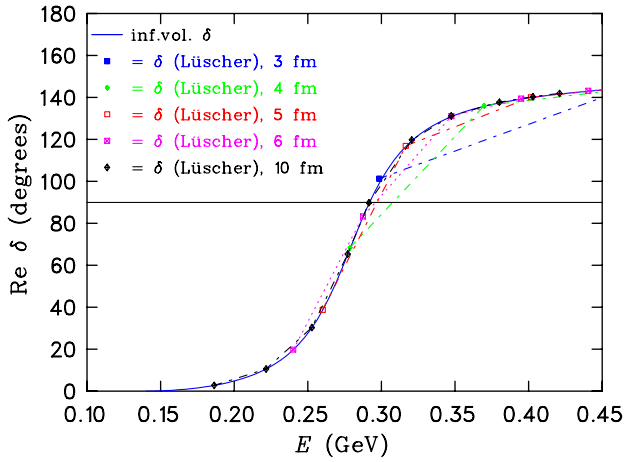
FIG. 4 (color online).   Estimates of the phase shift obtained from Lüscher's formula applied to the $\Delta \rightarrow N\pi$ model for a range of $L$ values. The infinite-volume phase shift is also shown as a solid line.
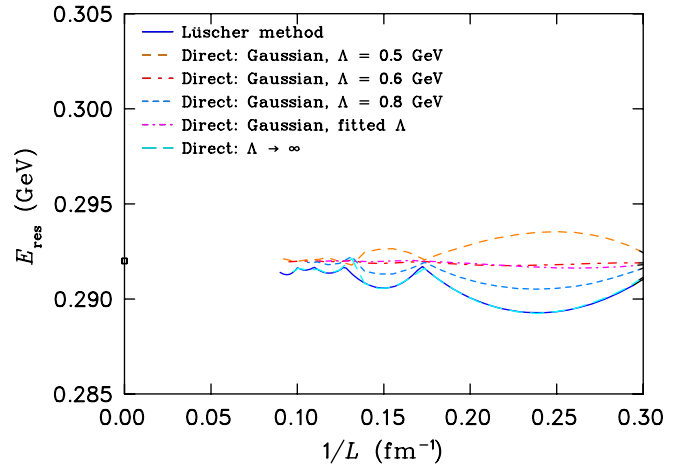


FIG. 5 (color online).   The resonance energy $E_{res}$ plotted against $1/L$. The experimental value is marked with a square. The results from fitting pseudodata with a different regulator, a Gaussian with $\Lambda = 0.5$, 0.6 and 0.8 GeV, or treating $\Lambda$ as a fit parameter, are plotted. The result of effectively removing the regulator (i.e., $\Lambda \rightarrow \infty$) is also shown. For comparison, the approach using Lüscher's method is marked with a solid line.

from the phase shift. The Breit-Wigner curve represents a suitable functional form,

$$e^{i\delta(k)} \sin \delta(k) = \frac{\tilde{\Gamma}(k)/2}{E - E_{res} - i\tilde{\Gamma}(k)/2}, \qquad (22)$$

where the width contains a cubic momentum factor, which yields the correct phase-space dependence for $l = 1$ [37],

$$\tilde{\Gamma}(k) = \frac{k^3}{k_{res}^3}\Gamma. \qquad (23)$$

To illustrate the comparison between Lüscher's method and the matrix Hamiltonian method, the pseudodata obtained from the $\Delta \rightarrow N\pi$ model will again be used. A modified version of the $\Delta \rightarrow N\pi$ model is constructed by replacing the regulator function $u(k_n)$ with a different form of regularization. First, a Gaussian regulator with a variety of values for the regularization scale $\Lambda$ will be considered. Using the $\Delta \rightarrow N\pi$ model, the closest two energy eigenvalues to the value of $E_{res}$, as estimated by Lüscher's formula, are chosen in order to constrain $\chi_\Delta$ and $\Delta_0$.

The behavior of the resonance energy $E_{res}$ may be plotted as a function of $1/L$, as shown in Fig. 5. A key observation is that the periodic deviations in the extraction of $E_{res}$ arise from the fact that, at certain volumes, an energy level may or may not lie near the resonance position (where $\delta = 90°$). That is, they are simply artefacts associated with the choice of interpolation. For box sizes where a discrete energy eigenvalue does lie near $E_{res}$, the experimental value is attained within a few MeV. This can provide a guide in choosing suitable box sizes for reliably reproducing the position of the $\Delta$ resonance.

It is also worth noting that the use of a Gaussian regulator, with $\Lambda \simeq 0.6$ GeV, provides a much more reliable reconstruction of the resonance position from the pseudodata than a low or high value of $\Lambda$. This is a consequence of

a close match between the underlying regulator of the pseudodata and the Gaussian regulator at this value of $\Lambda$. It provides evidence that a choice of regulator that correctly reflects the underlying phenomenology leads to a more stable identification of the resonance position. Nevertheless, even in the case of $\Lambda \rightarrow \infty$, which essentially corresponds to a dimensional regularization-like result [26], the matrix Hamiltonian method is just as successful as the Lüscher method.

Note that in Fig. 4 use of the Lüscher method results in an excellent agreement with the infinite-volume phase shift. However, at small volumes, the sparse distribution of energy eigenvalues leads to a difficulty in extracting the behavior at $\delta = 90°$. This accounts for the model dependence apparent in Fig. 5.

One might argue that the analysis of the pseudodata using a similar model that includes only the $\Delta \rightarrow N\pi$ couplings is ideally suited to the reconstruction method proposed above. In a more realistic scenario, a new pseudodata set is generated from a Hamiltonian model that now includes the effective contact interaction, introduced in Eq. (18). Again, a dipole regulator with $\Lambda = 0.8$ GeV is used. The energy levels of the new pseudodata are fitted to the more basic model using a Gaussian regulator, and the regularization scale $\Lambda$ is treated as an additional fit parameter. The behavior of the resonance energy versus $1/L$ is displayed in Fig. 6. The fitted values of $\Lambda$ in Fig. 5 are recalculated at each value of $L$, but they are typically close to 0.6 GeV, whereas in Fig. 6 the values are closer to 0.5 GeV. The tendency for slightly smaller fitted values of $\Lambda$ in Fig. 6 simply reflects the compensation of the regulator for the missing background interaction. For all regularization methods tested, the presence of a background interaction
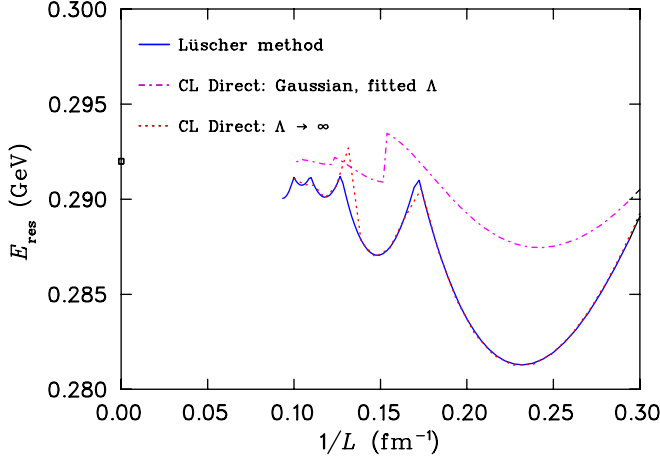
FIG. 6 (color online). The resonance energy $E_{\rm res}$ plotted against $1/L$, resulting from fitting pseudodata containing the nonresonant background interaction of Eq. (18). The experimental value is marked with a square. The result from fitting pseudodata with a Gaussian regulator is plotted, treating $\Lambda$ as a fit parameter. The result corresponding to $\Lambda \rightarrow \infty$ is also shown. Lüscher's approach is marked with a solid line.

also causes an exaggeration in the periodic deviations of $E_{\rm res}$ from interpolation. In all cases, the deviations are much larger due to the effect of the nonresonant background interaction. Nevertheless, a fairly reliable extraction of $E_{\rm res}$ is possible, if the energy eigenvalues lie close enough to the resonance energy. Most notably, there is significant improvement in the identification of $E_{\rm res}$ using the matrix Hamiltonian method if $\Lambda$ is treated as a fit parameter. This is remarkable, as it shows that the bare resonance mass, the coefficient of the interaction and the finite-range scale $\Lambda$ are collectively able to compensate for the missing $N\pi \leftrightarrow N\pi$ interactions; the underlying interactions are simply incorporated into the fit degrees of freedom.

## VI. ANALYSIS OF THE EIGENVECTORS

An analysis of the eigenvectors serves to emphasize a key feature of the Hamiltonian model. While only a single local operator describing the $\Delta$ resonance is included in the model, the interactions drive a significant coupling to all nearby lattice eigenstates. That is, one observes the generation of quantum mechanical admixtures of states from the interactions.

Consider the square of the overlap of each eigenvector with the bare state $|\Delta_0\rangle$, with a volume-dependent coefficient calculated from the following Jacobian:

$$dk^2 = \left(\frac{2\pi}{L}\right)^2 dn \tag{24}$$

$$= dE^2 = 2EdE, \tag{25}$$

$$\Rightarrow \int dn |\langle \Delta_0 | E_n \rangle|^2 = \int dE\, 2E \left(\frac{L}{2\pi}\right)^2 |\langle \Delta_0 | E \rangle|^2. \tag{26}$$
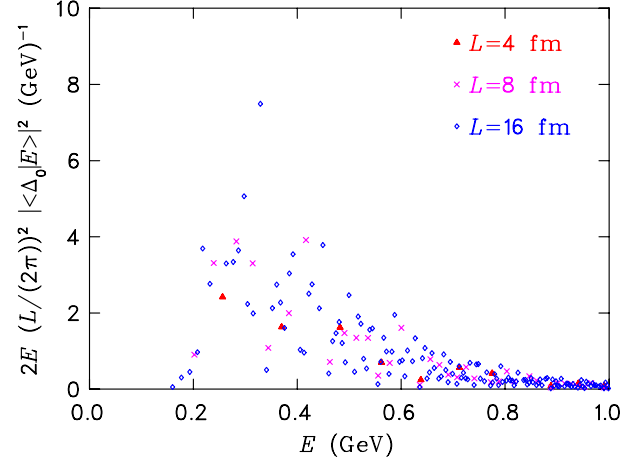


FIG. 7 (color online). The contribution of the eigenvectors to the bare $\Delta$ state in a finite volume, for a range of box sizes. The finite-volume Hamiltonian used includes the $N\pi \leftrightarrow N\pi$ interaction terms.

The result may be plotted as a function of external energy $E$. The peak of the resulting curve should lie at the value of the renormalized mass of the $\Delta$ baryon relative to the nucleon, 292 MeV. The result for the matrix Hamiltonian model, using a dipole regulator with $\Lambda = 0.8$ GeV, and including the Chew-Low-like background interactions from Eq. (18), is shown in Fig. 7. The magnitude of the contribution from the eigenvector spectrum to $\Delta_0$, $|\langle \Delta_0 | v \rangle|^2$, is shown for box sizes of 4, 8 and 16 fm. Over a broad range of energies, which dominate across the width of the resonance, it is evident that no single eigenstate, by itself, can be identified as either a local or a multihadron state. That is, the local, noninteracting $\Delta_0$ state couples to a range of low-lying states. This illustrates how early ideas from the heavier quark-mass domain, in distinguishing single-particle and multiparticle states, are no longer applicable in the light-quark regime of modern lattice simulations.

## VII. CONCLUSION

Finite-volume models provide key insights into the intrinsic attributes of lattice QCD. By examining the behavior of resonances and multiparticle states, one is able to identify more precisely the impact on a calculation associated with finite-volume effects.

By introducing a matrix Hamiltonian method, the finite-volume behavior near a resonance is reproducible. The avoided level crossings that indicate nontrivial mixing between single-particle and multiparticle states are also present in the model. Because the Hamiltonian is exactly solvable, the eigenvalue equation may be matched onto chiral effective field theory simply by a choice of coupling parameter for the potential. The Hamiltonian model can also be easily generalized to include multiple channels, in order to address more difficult scattering problems.

As a simple, introductory example, the $\Delta$ baryon resonance of $N\pi$ scattering was considered, and a method for extracting the phase shift from lattice QCD was developed. By matching the energy eigenstates of the model to those of a lattice calculation, the free parameters of the model were constrained, and their values were input into a scattering $t$-matrix equation, which uses chiral effective field theory. Initially, only the leading-order one-pion loop integral contribution to the resonance energy was included.

The method was tested in the context of a set of pseudodata generated by the $\Delta \to N\pi$ model. By considering a variety of different regularization scales, an indication of the model dependence in the calculation was found. A comparison was made with the well-known Lüscher method, and it was discovered that the matrix Hamiltonian method was at least comparable in reliability, with improvement when the regulator is a good approximation of the underlying phenomenology.

The extraction of the resonance parameters was investigated in a more realistic context, where nonresonant background interaction terms (corresponding to direct $N\pi \leftrightarrow N\pi$ scattering) were incorporated into the pseudodata. It was found that the $\Delta \to N\pi$ model was able to improve upon the Lüscher method, if the regularization scale was treated as an additional fit parameter. This indicates the ability of a bare resonance mass, a coupling scale, and regulator to compensate for underlying interactions that do not appear directly in the model. It also indicates that more complicated interactions may be effectively incorporated into the degrees of freedom of the model.

Thus the matrix Hamiltonian model, which uses an effective field theory style of approach, may indeed act as a guide to lattice QCD calculations in identifying the salient features derived from finite-volume effects, and the impact of the leading-order chiral contributions near a resonance. Though lattice QCD calculations are typically performed at pion masses heavier than the physical value, the avoided level crossing feature is expected to occur on the lattice when the pion-nucleon threshold appears below the $\Delta$ resonance. After considering some ideal pseudodata, the matrix Hamiltonian approach is well equipped to describe the behavior of actual lattice QCD results.

## ACKNOWLEDGMENTS

[1] R. G. Edwards, J. J. Dudek, D. G. Richards, and S. J. Wallace, Phys. Rev. D **84,** 074508 (2011).

[2] G. P. Engel, C. Lang, M. Limmer, D. Mohler, and A. Schafer [BGR (Bern-Graz-Regensburg) Collaboration], Phys. Rev. D **82,** 034505 (2010).

[3] M. S. Mahbub, W. Kamleh, D. B. Leinweber, P. J. Moran, and A. G. Williams (CSSM Lattice Collaboration), Phys. Lett. B **707,** 389 (2012).

[4] B. J. Menadue, W. Kamleh, D. B. Leinweber, and M. S. Mahbub, Phys. Rev. Lett. **108,** 112001 (2012).

[5] D. Mohler, Proc. Sci., LATTICE2012 (2012) 003.

[6] S. He, X. Feng, and C. Liu, J. High Energy Phys. 07 (2005) 011.

[7] V. Bernard, M. Lage, U.-G. Meißner, and A. Rusetsky, J. High Energy Phys. 08 (2008) 024.

[8] V. Bernard, D. Hoja, U.-G. Meißner, and A. Rusetsky, J. High Energy Phys. 06 (2009) 061.

[9] M. Döring and U.-G. Meißner, J. High Energy Phys. 01 (2012) 009.

[10] M. Döring, U.-G. Meißner, E. Oset, and A. Rusetsky, Eur. Phys. J. A **47,** 139 (2011).

[11] L. Roca and E. Oset, Phys. Rev. D **85,** 054507 (2012).

[12] P. Giudice, D. McManus, and M. Peardon, Phys. Rev. D **86,** 074516 (2012).

[13] S. Kreuzer and H. W. Grießhammer, Eur. Phys. J. A **48,** 93 (2012).

[14] M. Albaladejo, J. Oller, E. Oset, G. Rios, and L. Roca, J. High Energy Phys. 08 (2012) 071.

[15] J. J. Dudek, R. G. Edwards, and C. E. Thomas, Phys. Rev. D **87,** 034505 (2013).

[16] M. Gockeler, R. Horsley, M. Lage, U.-G. Meißner, P. E. L. Rakow, A. Rusetsky, G. Schierholz, and J. M. Zanotti, Phys. Rev. D **86,** 094513 (2012).

[17] M. Lüscher, Nucl. Phys. **B354,** 531 (1991).

[18] E. E. Jenkins and A. V. Manohar, In *Proceedings of Effective Field Theories of the Standard Model, Dobógokő, Hungary, 1991* (World Scientific, Singapore, 1992), pp. 113–137; Phys. Lett. B **259,** 353 (1991).

[19] E. E. Jenkins and A. V. Manohar, Phys. Lett. B **255,** 558 (1991).

[20] E. E. Jenkins, Nucl. Phys. **B368,** 190 (1992).

[21] J. N. Labrenz and S. R. Sharpe, Phys. Rev. D **54,** 4595 (1996).

[22] A. Walker-Loud, Nucl. Phys. **A747,** 476 (2005).

[23] P. Wang, D. B. Leinweber, A. W. Thomas, and R. D. Young, Phys. Rev. D **75,** 073012 (2007).

[24] V. Pascalutsa and M. Vanderhaeghen, Phys. Rev. D **73,** 034003 (2006).

[25] R. D. Young, D. B. Leinweber, and A. W. Thomas, Prog. Part. Nucl. Phys. **50,** 399 (2003).

[26] D. B. Leinweber, A. W. Thomas, and R. D. Young, Phys. Rev. Lett. **92**, 242002 (2004).

[27] D. B. Leinweber, A. W. Thomas, and R. D. Young, Nucl. Phys. **A755**, 59 (2005).

[28] J. Hall, D. Leinweber, and R. Young, Phys. Rev. D **82**, 034010 (2010).

[29] J. M. M. Hall, F. X. Lee, D. B. Leinweber, K. F. Liu, N. Mathur, R. D. Young, and J. B. Zhang, Phys. Rev. D **84**, 114011 (2011).

[30] S. Theberge, A. W. Thomas, and G. A. Miller, Phys. Rev. D **22**, 2838 (1980).

[31] A. W. Thomas, S. Theberge, and G. A. Miller, Phys. Rev. D **24**, 216 (1981).

[32] T. Mongan, Phys. Rev. **178**, 1597 (1969).

[33] C. Liu, X. Feng, and S. He, Int. J. Mod. Phys. A **21**, 847 (2006).

[34] V. Bernard, D. Hoja, U. Meißner, and A. Rusetsky, J. High Energy Phys. 09 (2012) 023.

[35] M. Doring, U. Meißner, E. Oset, and A. Rusetsky, Eur. Phys. J. A **48**, 114 (2012).

[36] M. T. Hansen and S. R. Sharpe, Phys. Rev. D **86**, 016007 (2012).

[37] J. M. Blatt and W. F. Weisskopf, *Theoretical Nuclear Physics* (John Wiley & Sons, New York, 1952).